Electronic Supporting Information

Crystal engineering of monometallic lanthanide(III) supramolecular systems within the N_3-tridentate hydrazone Schiff-base ligand

Dominika Prętka[a], Dawid Marcinkowski[a], Agnieszka Siwiak[a], Maciej Kubicki[a], Giuseppe Consiglio[b], Violetta Patroniak[a], Adam Gorczyński[a*]*

[a]Faculty of Chemistry, Adam Mickiewicz University in Poznań, Uniwersytetu Poznańskiego 8, 61-614 Poznań, Poland;

[b]Dipartimento di Scienze Chimiche, Università di Catania, I-95125 Catania, Italy;

Table of content

Synthetic procedures details and characterization of the lanthanide complexes

Complexes obtained from Ln(OTf)$_3$ salts. To a solution of **L** (40.0 mg, 0.18 mmol) in the mixture of MeOH/MeCN (1:1 v:v) appropriate metal salt (0.09 mmol) was added (La(CF_3SO_3)$_3$ - **1**, Pr(CF_3SO_3)$_3$ - **2**, Nd(CF_3SO_3)$_3$ - **3**, Sm(CF_3SO_3)$_3$ - **4**, Eu(CF_3SO_3)$_3$ - **5**, Gd(CF_3SO_3)$_3$ - **6**, Tb(CF_3SO_3)$_3$ - **7**, Dy(CF_3SO_3)$_3$ - **8**, Ho(CF_3SO_3)$_3$ - **9,** Er(CF_3SO_3)$_3$ - **10**, Yb(CF_3SO_3)$_3$ - **11** and Lu(CF_3SO_3)$_3$ - **12**. Upon mixing, the reaction mixtures instantly produced yellow solutions, which were stirred for 24 hours at room temperature. Subsequently, the solvents were evaporated under reduced pressure, resulting in residues that were dissolved in the smallest possible amount of a mixture containing methanol and acetonitrile in a 1:1 volume ratio. The dissolved residues were then precipitated by adding an excess of Et_2O. The resulting yellow solids were filtered using suction filtration and subsequently dried under vacuum.

[La**L**$_2$(OTf)$_3$] (***1***)

Yield: 55.0 mg, 58.2%. Crystals suitable for X-ray analysis were obtained *via* slow diffusion methods in MeOH, MeCN/iPr_2O system at 4°C. IR (KBr, cm^{-1}): ν(C-H)$_{arom}$ 3126; $\nu_{as}(CH_3)$2960; $\nu_s(CH_3)$ 2894; ν(C=C) 1610, 1591, 1571, 1502; ν(C=N) 1442, 1331; $\delta(CH_3)$ 1382; $\nu_{as}(SO_3)$ 1310; $\nu_{as}(CF_3)$ 1245, 1220; $\nu_s(CF_3)$ 1164; $\nu_s(SO_3)$ 1035; γ(C-H)$_{arom}$ 1003, 888, 770. ESI-MS(+) m/z (%): 216 (100) $[LH]^+$, 652 (10) $[LaL(CF_3SO_3)_2]^+$, 867 (10) $[LaL_2(CF_3SO_3)_2]^+$.

[Pr**L**$_2$(OTf)$_3$] (***2***)

Yield: 53.0 mg, 56.0%. Crystals suitable for X-ray analysis were obtained *via* slow diffusion methods in MeOH/iPr_2O system at 4°C. IR (KBr, cm^{-1}): ν(C-H)$_{arom}$ 3127; $\nu_{as}(CH_3)$ 2956; $\nu_s(CH_3)$ 2894; ν(C=C) 1610, 1585, 1502; ν(C=N) 1439, 1327; $\delta(CH_3)$ 1380; $\nu_{as}(SO_3)$ 1305; $\nu_{as}(CF_3)$ 1246, 1220; $\nu_s(CF_3)$ 1158; $\nu_s(SO_3)$ 1036; γ(C-H)$_{arom}$ 1002, 961, 888, 772. ESI-MS(+) m/z (%): 216 (100) $[LH]^+$, 536 (100) $[PrL(CF_3SO_3)(CH_3OH)-H^+]^+$, 869 (10) $[PrL_2(CF_3SO_3)_2]^+$.

[Pr**L**$_2$(OTf)$_3$](MeCN) (***2α***)

Yield: 54.2 mg, 56.0%. Crystals suitable for X-ray analysis were obtained *via* slow diffusion methods in MeOH, MeCN/iPr_2O system at 4°C. IR (KBr, cm^{-1}): ν(C-H)$_{arom}$ 3144; $\nu_{as}(CH_3)$ 2959; $\nu_s(CH_3)$ 2896; ν(C=C) 1610, 1587, 1506; ν(C=N) 1447, 1327; $\delta(CH_3)$ 1378; $\nu_{as}(SO_3)$ 1301; $\nu_{as}(CF_3)$ 1247, 1221; $\nu_s(CF_3)$ 1163; $\nu_s(SO_3)$ 1035; γ(C-H)$_{arom}$ 1002, 964, 891, 776. ESI-MS(+) m/z (%): 216 (100) $[LH]^+$, 869 (10) $[PrL_2(CF_3SO_3)_2]^+$.

[Nd**L**$_2$(OTf)$_3$] (***3***)

Yield: 62.5 mg 65.8%. Crystals suitable for X-ray analysis were obtained *via* slow diffusion methods in MeOH, MeCN/iPr_2O system at 4°C. IR (KBr, cm^{-1}): ν(C-H)$_{arom}$ 3129; $\nu_{as}(CH_3)$ 2957; $\nu_s(CH_3)$ 2899; ν(C=C) 1611, 1588, 1502; ν(C=N) 1445, 1329; $\delta(CH_3)$ 1380; $\nu_{as}(SO_3)$ 1303; $\nu_{as}(CF_3)$ 1247, 1219; $\nu_s(CF_3)$ 1163; $\nu_s(SO_3)$ 1036; γ(C-H)$_{arom}$ 1004, 889, 772. ESI-MS(+) m/z (%): 216 (90) $[LH]^+$, 655 (15) $[Nd\mathbf{L}(CF_3SO_3)_2]^+$.

[Sm**L**$_2$(OTf)$_3$] (***4***)

Yield: 60.8 mg, 63.6%. Crystals suitable for X-ray analysis were obtained *via* slow diffusion methods in MeOH, MeCN/iPr_2O system at 4°C. IR (KBr, cm^{-1}): ν(C-H)$_{arom}$ 3127; $\nu_{as}(CH_3)$ 2956; $\nu_s(CH_3)$ 2896; ν(C=C) 1610, 1590, 1502; ν(C=N) 1442, 1328; $\delta(CH_3)$ 1381; $\nu_{as}(SO_3)$ 1305; $\nu_{as}(CF_3)$ 1237, 1220; $\nu_s(CF_3)$ 1164; $\nu_s(SO_3)$ 1033; γ(C-H)$_{arom}$ 1004, 889, 775. ESI-MS(+) m/z (%): 216 (100) $[LH]^+$, 547 (90) $[SmL_2(CF_3SO_3)(CH_3OH)-H^+]^+$, 880 (20) $[SmL_2(CF_3SO_3)]^+$.

[Eu**L**$_2$(OTf)$_3$] (***5***)

Yield: 72.5 mg, 75.7%. Crystals suitable for X-ray analysis were obtained *via* slow diffusion methods in MeOH/iPr_2O system at 4°C. IR (KBr, cm^{-1}): ν(C-H)$_{arom}$ 3127; $\nu_{as}(CH_3)$ 2962; $\nu_s(CH_3)$ 2924; ν(C=C) 1609, 1590, 1497; ν(C=N) 1442, 1327; $\delta(CH_3)$ 1381; $\nu_{as}(SO_3)$ 1285; $\nu_{as}(CF_3)$ 1247, 1224; $\nu_s(CF_3)$ 1167; $\nu_s(SO_3)$ 1028; γ(C-H)$_{arom}$ 1004, 963, 885, 771. ESI-MS(+) m/z (%): 216 (100) $[LH]^+$, 548 (100) $[EuL(CF_3SO_3)(CH_3OH)-H^+]^+$, 881 (10) $[EuL_2(CF_3SO_3)_2]^+$.

[Gd**L**$_2$(OTf)$_3$] (***6***)

Yield: 52.9 mg, 55.0%. Crystals suitable for X-ray analysis were obtained *via* slow diffusion methods in MeOH/iPr_2O system at 4°C. IR (KBr, cm^{-1}): ν(C-H)$_{arom}$ 3127; $\nu_{as}(CH_3)$ 2964; $\nu_s(CH_3)$ 2898; ν(C=C) 1611, 1589, 1497; ν(C=N) 1439, 1323; $\delta(CH_3)$ 1378; $\nu_{as}(SO_3)$ 1280; $\nu_{as}(CF_3)$ 1252, 1223; $\nu_s(CF_3)$ 1167; $\nu_s(SO_3)$ 1029; γ(C-H)$_{arom}$ 1004, 885, 769. ESI-MS(+) m/z (%): 216 (100) $[LH]^+$, 368 (30) $[GdL_2(CF_3SO_3)]^{2+}$, 886 (20) $[GdL_2(CF_3SO_3)_2]^+$.

[Tb**L**$_2$(MeOH)$_2$(OTf)](OTf)$_2$ (***7***)

Yield: 68.9 mg, 64.4%. Crystals suitable for X-ray analysis were obtained *via* slow diffusion methods in MeOH/iPr_2O system at 4°C. IR (KBr, cm^{-1}): ν(C-H)$_{arom}$ 3127; $\nu_{as}(CH_3)$ 2960; $\nu_s(CH_3)$ 2897; ν(C=C) 1610, 1590, 1501; ν(C=N) 1440, 1329; $\delta(CH_3)$ 1380; $\nu_{as}(SO_3)$ 1300; $\nu_{as}(CF_3)$ 1241, 1218; $\nu_s(CF_3)$ 1167; $\nu_s(SO_3)$ 1025; γ(C-H)$_{arom}$

1004, 965, 888, 773. ESI-MS(+) m/z (%): 216 (95) $[LH]^+$, 554 (20) $[TbL(CF_3SO_3)(CH_3OH)-H^+]^+$, 887 (15) $[TbL_2(CF_3SO_3)_2]^+$.

[Tb**L**$_2$(OTf)$_2$(MeCN)](OTf) (***7a***)

Yield: 64.3 mg, 64.4%. Crystals suitable for X-ray analysis were obtained *via* slow diffusion methods in MeCN/iPr_2O system at 4°C. IR (KBr, cm^{-1}): ν(C-H)$_{arom}$ 3129; $\nu_{as}(CH_3)$ 2959; $\nu_s(CH_3)$ 2938; ν(C=C) 1611, 1591, 1499; ν(C=N) 1442, 1328; $\delta(CH_3)$ 1380; $\nu_{as}(SO_3)$ 1300; $\nu_{as}(CF_3)$ 1239, 1221; $\nu_s(CF_3)$ 1169; $\nu_s(SO_3)$ 1030; γ(C-H)$_{arom}$ 1006, 966, 886, 772. ESI-MS(+) m/z (%): 216 (100) $[LH]^+$, 671 (35) $[TbL(CF_3SO_3)_2]^+$, 887 (30) $[TbL_2(CF_3SO_3)_2]^+$.

[Dy**L**$_2$(MeOH)$_2$(OTf)](OTf)$_2$ (***8***)

Yield: 61.6 mg, 60.0%. Crystals suitable for X-ray analysis were obtained *via* slow diffusion methods in MeOH/iPr_2O system at 4°C. IR (KBr, cm^{-1}): ν_{broad}(O-H)$_{methanol}$ 3404; ν(C-H)$_{arom}$ 3127; $\nu_{as}(CH_3)$ 2960; $\nu_s(CH_3)$ 2900; ν(C=C) 1609, 1590, 1497; ν(C=N) 1438, 1326; $\delta(CH_3)$ 1379; $\nu_{as}(SO_3)$ 1303; $\nu_{as}(CF_3)$ 1231, 1222; $\nu_s(CF_3)$ 1169; $\nu_s(SO_3)$ 1029; γ(C-H)$_{arom}$ 1004, 963, 888, 768. ESI-MS(+) m/z (%): 216 (100) $[LH]^+$, 559 (60) $[DyL_2(CF_3SO_3)_3+2K^+]^{2+}$, 676 (20) $[DyL(CF_3SO_3)_2]^+$, 892 (10) $[DyL_2(CF_3SO_3)_2]^+$.

[Ho**L**$_2$(OTf)$_2$(MeCN)](OTf) (***9***)

Yield: 63.3 mg, 62.8%. Crystals suitable for X-ray analysis were obtained *via* slow diffusion methods in MeOH, MeCN/iPr_2O system at 4°C. IR (KBr, cm^{-1}):; ν(C-H)$_{arom}$ 3136; $\nu_{as}(CH_3)$ 2963; $\nu_s(CH_3)$ 2919; ν(C=C) 1664, 1614, 1591, 1500; ν(C=N) 1444, 1327; $\delta(CH_3)$ 1379; $\nu_{as}(SO_3)$ 1291; $\nu_{as}(CF_3)$ 1242, 1221; $\nu_s(CF_3)$ 1168; $\nu_s(SO_3)$ 1025; γ(C-H)$_{arom}$ 1007, 966, 888, 768. ESI-MS(+) m/z (%): 216 (100) $[LH]^+$, 560 (30) $[HoL_2(CF_3SO_3)_3+2K^+]^{2+}$, 678 (15) $[HoL(CF_3SO_3)_2]^+$, 893 (10) $[HoL_2(CF_3SO_3)_2]^+$.

[Er**L**$_2$(OTf)$_2$(MeOH)$_2$](OTf)$_2$ (***10***)

Yield: 63.3 mg, 54.2%. Crystals suitable for X-ray analysis were obtained *via* slow diffusion methods in MeOH/iPr_2O system at 4°C. IR (KBr, cm^{-1}): ν_{broad}(OH)$_{methanol}$ 3438; ν(C-H)$_{arom}$ 3025; ν_{as}(C-H)$_{aliph}$ 2983; ν_s(C-H)$_{aliph}$ 2947; ν(C=C) 1677, 1614, 1504; ν(C=N) 1443, 1328; $\delta(CH_3)$ 1383; $\nu_{as}(SO_3)$ 1293; $\nu_{as}(CF_3)$ 1256, 1245; $\nu_s(CF_3)$ 1172; $\nu_s(SO_3)$ 1030; γ(C-H)$_{arom}$ 1023, 997, 889, 776. ESI-MS(+) m/z (%): 216 (100) $[LH]^+$, 431 (15) $[(HL)_2]^+$, 679 (10) $[ErL(CF_3SO_3)_2]^+$.

[Yb**L**$_2$(OTf)$_2$](OTf) (***11***)

Yield: 54.7 mg, 56.0%. Crystals suitable for X-ray analysis were obtained *via* slow diffusion methods in MeCN/iPr$_2$O system at 4°C. IR (KBr, cm^{-1}): ν_{broad}(OH)$_{methanol}$ 3467; ν(C-H)$_{arom}$ 3147; ν_{as}(C-H)$_{aliph}$ 2984; ν_s(C-H)$_{aliph}$ 2936; ν(C=C) 1602, 1566; ν(C=N) 1466, 1318; δ(CH$_3$) 1363; ν_{as}(SO$_3$) 1289; ν_{as}(CF$_3$) 1247, 1221; ν_s(CF$_3$) 1161; ν_s(SO$_3$) 1027; γ(C-H)$_{arom}$ 986, 869, 799, 749. ESI-MS(+) m/z (%): 216 (100) [HL]$^+$, 687 (30) [YbL(CF$_3$SO$_3$)$_2$]$^+$, 902 (40) [YbL$_2$(CF$_3$SO$_3$)$_2$]$^+$.

[Lu**L**$_2$(OTf)$_3$] (**12**)

Yield: 55.9 mg, 57.8%. IR (KBr, cm^{-1}): ν(C-H)$_{arom}$ 3130; ν_{as}(C-H)$_{aliph}$ 2967; ν_s(C-H)$_{aliph}$ 2926; ν(C=C) 1616, 1591, 1570, 1501; ν(C=N) 1440, 1330; δ(CH$_3$) 1380; ν_{as}(SO$_3$) 1278; ν_{as}(CF$_3$) 1223; ν_s(CF$_3$) 1167; ν_s(SO$_3$) 1030; γ(C-H)$_{arom}$ 1007, 861, 885, 770. ESI-MS(+) m/z (%): 216 (100) [LH]$^+$, 570 (10) [LuL(CF$_3$SO$_3$)(CH$_3$OH)−H$^+$]$^+$, 269 (5) [LuL(CF$_3$SO$_3$)]$^{2+}$. ^{1}H NMR (600 MHz, Acetonitrile-*d*$_3$) δ, ppm: 8.61 (1H), 8.02 (1H), 7.97 (1H), 7.38 (1H), 7.29 (1H), 7.27 (1H), 7.17 (1H), 3.92 (3H), 3.63 (3H). 3.61 (d, 3H).

Complexes obtained from Ln(NO$_3$)$_3$ salts. For complexes **13-25** the molar ratio of the ligand to the corresponding salt was 1:1. To a solution of **L** (40.0 mg, 0.18 mmol) in the mixture of MeOH/MeCN (1:1 v:v) appropriate metal salt (0.18 mmol) was added (La(NO$_3$)$_3$·6H$_2$O - **13**, Pr(NO$_3$)$_3$·6H$_2$O - **14**, Nd(NO$_3$)$_3$·6H$_2$O - **15**, Sm(NO$_3$)$_3$·6H$_2$O - **16**, Eu(NO$_3$)$_3$·5H$_2$O - **17**, Gd(NO$_3$)$_3$·6H$_2$O - **18**, Tb(NO$_3$)$_3$·5H$_2$O - **19**, Dy(NO$_3$)$_3$·6H$_2$O - **20**, Ho(NO$_3$)$_3$·5H$_2$O - **21**, Er(NO$_3$)$_3$·5H$_2$O - **22**, Tm(NO$_3$)$_3$·5H$_2$O - **23**, Yb(NO$_3$)$_3$·5H$_2$O - **24** and Lu(NO$_3$)$_3$·8DMSO - **25**. Subsequently, the solvents were evaporated under reduced pressure, resulting in residues that were dissolved in the smallest possible amount of a mixture containing methanol and acetonitrile in a 1:1 volume ratio. The dissolved residues were then precipitated by adding an excess of Et$_2$O or iPr$_2$O. The resulting yellow solids were filtered using suction filtration and subsequently dried under vacuum.

[La**L**(NO$_3$)$_3$(MeOH)](MeCN) (***13***)

Yield: 70.7 mg, 62.0%. Crystals suitable for X-ray analysis were obtained *via* slow diffusion methods in MeOH, MeCN/iPr$_2$O system at 4°C. IR (KBr, cm^{-1}): ν_{broad}(O-H)$_{methanol}$ 3387; ν(C-H)$_{arom}$ 3118; ν_{as}(CH$_3$) 2974; ν_s(CH$_3$) 2924; ν(C=C) 1606, 1580; ν_{as}(NO$_2$) 1497, 1453; ν(C=N) 1433, 1318; δ(CH$_3$) 1384; $\nu_{s,broad}$(NO$_2$) 1284, 1232; ν(NO) 1042; γ(C-H)$_{arom}$ 1002, 955, 885, 768; δ(NO) 817. ESI-MS(+) m/z (%): 216 (100) [LH]$^+$, 239 (10) [LaL(NO$_3$)$_2$+H$^+$]$^{2+}$, 478 (10) [LaL(NO$_3$)$_2$]$^+$.

[Pr**L**$(NO_3)_3$(MeOH)](MeOH) (***14***)

Yield: 65.4 mg, 59.6%. Crystals suitable for X-ray analysis were obtained *via* slow diffusion methods in MeOH, MeCN/iPr_2O system at 4°C. IR (KBr, cm^{-1}): ν_{broad}(O-H)$_{methanol}$ 3430; ν(C-H)$_{arom}$ 3127 $\nu_{as}(CH_3)$ 2957; $\nu_s(CH_3)$ 2923; ν(C=C) 1632, 1609, 1583; $\nu_{as}(NO_2)$ 1496 ; ν(C=N) 1436, 1318; $\delta(CH_3)$ 1385; $\nu_{s,broad}(NO_2)$ 1288, 1233; ν(NO) 1060; γ(C-H)$_{arom}$ 1034, 1002, 885, 773; δ(NO) 817. ESI-MS(+) m/z (%): 216 (100) $[LH]^+$, 480 (90) $[PrL(NO_3)_2]^+$, 695 (20) $[PrL_2(NO_3)_2]^+$.

[Nd**L**$(NO_3)_3$(MeOH)](MeCN) (***15***)

Yield: 80.6 mg, 70.1%. Crystals suitable for X-ray analysis were obtained *via* slow diffusion methods in MeOH, MeCN/iPr_2O system at 4°C. IR (KBr, cm^{-1}): ν_{broad}(O-H)$_{methanol}$ 3432; ν(C-H)$_{arom}$ 3128 $\nu_{as}(CH_3)$ 2960; $\nu_s(CH_3)$ 2927; ν(C=C) 1671, 1610, 1586; $\nu_{as}(NO_2)$ 1497 ; ν(C=N) 1436, 1322; $\delta(CH_3)$ 1387; $\nu_{s,broad}(NO_2)$ 1278 1234 ; ν(NO) 1051; γ(C-H)$_{arom}$ 1034, 1006, 883, 771; δ(NO) 816. ESI-MS(+) m/z (%): 216 (100) $[LH]^+$, 251 (10) $[NdL(NO_3)_2+Na^+]^{2+}$, 481 (10) $[NdL(NO_3)_2]^+$.

[Sm**L**$(NO_3)_3(H_2O)$](MeOH) (***16***)

Yield: 73.1 mg, 65.3%. Crystals suitable for X-ray analysis were obtained *via* slow diffusion methods in MeOH/iPr_2O system at 4°C. IR (KBr, cm^{-1}): ν_{broad}(O-H)$_{methanol}$ 3426; ν(C-H)$_{arom}$ 3127 $\nu(CH_3)$ 2962 $\nu_s(CH_3)$ 2930 ν(C=C) 1672, 1633, 1610, 1590; $\nu_{as}(NO_2)$ 1497; ν(C=N) 1440, 1322; $\delta(CH_3)$ 1382; $\nu_{s,broad}(NO_2)$ 1286, 1232; ν(NO) 1049; γ(C-H)$_{arom}$ 1034, 1005, 881, 769; δ(NO) 812. ESI-MS(+) m/z (%): 214 (25) $[SmL(NO_3)]^{2+}$, 216 (100) $[LH]^+$, 491 (20) $[SmL(NO_3)_2]^+$.

[Eu**L**$(NO_3)_3(H_2O)$](MeOH) (***17***)

Yield: 88.5 mg, 78.9%. Crystals suitable for X-ray analysis were obtained *via* slow diffusion methods in MeOH/iPr_2O system at 4°C. IR (KBr, cm^{-1}): ν_{broad}(O-H)$_{methanol}$ 3428; ν(C-H)$_{arom}$ 3122 $\nu_{as}(CH_3)$ 2962; $\nu_s(CH_3)$ 2926; ν(C=C) 1671, 1635, 1610, 1587; $\nu_{as}(NO_2)$ 1499 ; ν(C=N) 1438, 1321; $\delta(CH_3)$ 1384; $\nu_{s,broad}(NO_2)$ 1283, 1236; ν(NO) 1060; γ(C-H)$_{arom}$ 1034, 1003, 884, 770; δ(NO) 814. ESI-MS(+) m/z (%): 216 (100) $[LH]^+$, 429 (10) $[EuL(NO_3)\text{-}H^+]^+$, 492 (45) $[EuL(NO_3)_2]^+$.

[Gd**L**$(NO_3)_3$(MeOH)](MeCN) (***18***)

Yield: 72.7 mg, 61.9%. Crystals suitable for X-ray analysis were obtained *via* slow diffusion methods in MeOH, MeCN/iPr_2O system at 4°C. IR (KBr, cm^{-1}): ν_{broad}(O-H)$_{methanol}$ 3428; ν(C-H)$_{arom}$ 3126; $\nu_{as}(CH_3)$ 2954; $\nu_s(CH_3)$

2931; ν(C=C) 1672, 1609; $\nu_{as}(NO_2)$ 1497, 1460; ν(C=N) 1437, 1322; $\delta(CH_3)$ 1384; $\nu_{s,broad}(NO_2)$ 1286, 1237; ν(NO) 1046; $\gamma(C\text{-}H)_{arom}$ 1007, 885, 773, 743; δ(NO) 815. ESI-MS(+) m/z (%): 216 (100) $[LH]^+$, 249 (10) $[GdL(NO_3)_2+H^+]^{2+}$, 497 (25) $[GdL(NO_3)_2]^+$.

[Tb**L**$(NO_3)_3(H_2O)$](MeOH) (***19***)

Yield: 82.5 mg, 72.7%. Crystals suitable for X-ray analysis were obtained *via* slow diffusion methods in MeOH, MeCN/iPr_2O system at 4°C. IR (KBr, cm^{-1}): $\nu_{broad}(O\text{-}H)_{methanol}$ 3391; $\nu(C\text{-}H)_{arom}$ 3147; $\nu_{as}(CH_3)$ 2962; $\nu_s(CH_3)$ 2923; ν(C=C) 1665, 1611, 1586; $\nu_{as}(NO_2)$ 1497; ν(C=N) 1435, 1325; $\delta(CH_3)$ 1384; $\nu_{s,broad}(NO_2)$ 1289, 1234; ν(NO) 1051; $\gamma(C\text{-}H)_{arom}$ 1027, 1004, 883, 772; δ(NO) 811. ESI-MS(+) m/z (%): 216 (70) $[LH]^+$, 315 (100) $[TbL(NO_3)_3(H_2O)_2(CH_3OH)+2H^+]^{2+}$, 498 (45) $[TbL(NO_3)_2]^+$.

[Dy**L**$(NO_3)_3(H_2O)$](MeOH) (***20***)

Yield: 73.3 mg, 64.2%. Crystals suitable for X-ray analysis were obtained *via* slow diffusion methods in MeOH/iPr_2O system at 4°C. IR (KBr, cm^{-1}): $\nu_{broad}(O\text{-}H)_{methanol}$ 3374; $\nu(C\text{-}H)_{arom}$ 3118; $\nu_{as}(CH_3)$ 2959; $\nu_s(CH_3)$ 2932; ν(C=C) 1615, 1589, 1570; $\nu_{as}(NO_2)$ 1497; ν(C=N) 1437, 1322; $\delta(CH_3)$ 1384; $\nu_{s,broad}(NO_2)$ 1291, 1238; ν(NO) 1049; $\gamma(C\text{-}H)_{arom}$ 1002, 885, 769; δ(NO) 812. ESI-MS(+) m/z (%): 216 (100) $[LH]^+$, 317 (30) $[DyL(NO_3)_3(H_2O)_2(CH_3OH)+2H^+]^{2+}$, 502 (20) $[DyL(NO_3)_2]^+$.

[Ho**L**$(NO_3)_3$(MeOH)](MeCN) (***21***)

Yield: 78.5 mg, 66.0%. Crystals suitable for X-ray analysis were obtained *via* slow diffusion methods in MeOH, MeCN/iPr_2O system at 4°C. IR (KBr, cm^{-1}): $\nu_{broad}(O\text{-}H)_{methanol}$ 3397; $\nu(C\text{-}H)_{arom}$ 3143; $\nu_{as}(CH_3)$ 2959; $\nu_s(CH_3)$ 2924; ν(C=C) 1667, 1611, 1588; $\nu_{as}(NO_2)$ 1497; ν(C=N) 1436, 1325; $\delta(CH_3)$ 1384; $\nu_{s,broad}(NO_2)$ 1290, 1236; ν(NO) 1051; $\gamma(C\text{-}H)_{arom}$ 1007, 881, 772, 746; δ(NO) 811. ESI-MS(+) m/z (%): 216 (100) $[LH]^+$, 321 (45) $[HoL(NO_3)_3(CH_3CN)(CH_3OH)+2H^+]^{2+}$, 504 (20) $[HoL(NO_3)_2]^+$.

[Er**L**$(NO_3)_3(H_2O)$] (***22***)

Yield: 67.4 mg, 62.0%. Crystals suitable for X-ray analysis were obtained *via* slow diffusion methods in MeOH/iPr_2O system at 4°C. IR (KBr, cm^{-1}): $\nu_{broad}(OH)_{methanol}$ 3426; $\nu(C\text{-}H)_{arom}$ 3147; $\nu_{as}(C\text{-}H)_{aliph}$ 2985; $\nu_s(C\text{-}H)_{aliph}$ 2972; ν(C=C) 1670, 1613, 1540; $\nu_{as}(NO_2)$ 1460, 1450; ν(C=N) 1439, 1325; $\delta(CH_3)$ 1384; $\nu_{s,\,broad}(NO_2)$ 1295, 1237; ν(NO) 1051; $\gamma(C\text{-}H)_{arom}$ 1110, 1030, 1006, 997, 882, 773; δ(NO) 811. ESI-MS(+) m/z (%): 216 (100) $[LH]^+$, 199 (10) $[ErL(H_2O)\text{-}H^+]^{2+}$, 230 (10) $[ErL(NO_3)(H_2O)]^{2+}$, 253 (10) $[ErL(NO_3)_2+H^+]^{2+}$.

[Tm**L**$(NO_3)_3$(MeOH)](NO_3)(**L**) (***23***)

Yield: 101.5 mg, 62.0%. Crystals suitable for X-ray analysis were obtained *via* slow diffusion methods in MeOH, MeCN/iPr_2O system at 4°C. IR (KBr, cm^{-1}): $\nu_{broad}(O\text{-}H)_{methanol}$ 3396; $\nu(C\text{-}H)_{arom}$ 3144 $\nu_{as}(CH_3)$ 2955; $\nu_s(CH_3)$ 2923; ν(C=C) 1668, 1615, 1589; $\nu_{as}(NO2)$ 1500 ; ν(C=N) 1438, 1322; $\delta(CH_3)$ 1383; $\nu_{s,broad}(NO_2)$ 1298, 1238; ν(NO) 1050; $\gamma(C\text{-}H)_{arom}$ 1031, 1007, 881, 772; δ(NO) 810. ESI-MS(+) m/z (%): 216 (70) $[LH]^+$, 362 (5) $[TmL_2(NO_3)_2{+}H^+]^{2+}$, 508 (10) $[TmL(NO_3)_2]^+$.

[Yb**L**$(NO_3)_3$(MeOH)](MeCN) (***24***)

Yield: 77.4 mg, 65.0%. Crystals suitable for X-ray analysis were obtained *via* slow diffusion methods in MeCN/iPr_2O system at 4°C. IR (KBr, cm^{-1}): $\nu_{broad}(OH)_{methanol}$ 3422; $\nu(C\text{-}H)_{arom}$ 3091; $\nu_{as}(C\text{-}H)_{aliph}$ 2992; $\nu_s(C\text{-}H)_{aliph}$ 2973; ν(C=C) 1668, 1614, 1503; $\nu_{as}(NO_2)$ 1461, 1450; ν(C=N) 1439, 1325; $\delta(CH_3)$ 1384; $\nu_{s,\,broad}(NO_2)$ 1297, 1238; ν(NO) 1051; $\gamma(C\text{-}H)_{arom}$ 1111, 1031, 1007, 995, 881, 773, 713; δ(NO) 811. ESI-MS(+) m/z (%): 216 (100) $[LH]^+$, 242 (20) $[YbL(NO_3)(MeOH)]^{2+}$, 273 (10) $[YbL(NO_3)_2(MeOH){+}H]^{2+}$.

[Lu**L**$(NO_3)_3$(DMSO)](MeCN) (***25***)

Yield: 74.5 mg, 61.2%. Crystals suitable for X-ray analysis were obtained via slow diffusion methods in MeOH, MeCN/iPr_2O system at 4°C. IR (KBr, cm^{-1}) $\nu(C\text{-}H)_{arom}$ 3121; $\nu_{as}(C\text{-}H)_{aliph}$ 2960; $\nu_s(C\text{-}H)_{aliph}$ 2925; ν(C=C) 1616, 1588; $\nu_{as}(NO2)$ 1506; ν(C=N) 1440, 1331; δ(CH3) 1387; $\nu_{s,broad}(NO2)$ 1288, 1243; ν(NO) 1047; $\gamma(C\text{-}H)_{arom}$ 1031, 1003, 886, 765; δ(NO) 814. ESI-MS(+) m/z (%): 216 (100) $[LH]^+$, 514 (20) $[LuL(NO_3)_2]^+$, 278 (10) $[LuL(NO_3)(MeOH)_2(MeCN)]^{2+}$. ^1H NMR (600 MHz, Acetonitrile-d_3) δ, ppm: 8.60 – 8.56 (1H), 7.97 – 7.93 (1H), 7.90 (1H), 7.22 (1H), 7.19 (1H), 7.13 – 7.11 (2H), 3.87 (3H), 3.62 – 3.60 (3H).

Supporting Tables

Table S1. Crystallographic data and structure refinement details of ligand **LH·Br$^-$.**

LH·Br$^-$: $C_{11}H_{14}N_5^+ \cdot Br^- \cdot CH_3OH$, M_r=328.22, triclinic, $P\bar{1}$, a=7.1754(4)Å, b=9.5801(5)Å, c=11.4950(6)Å, V=704.82(7)Å^3, Z=2, d_x=1.547 g·cm^{-3}, F(000)=336, μ=3.990mm^{-1}, 4875 reflections collected, of which 2784 unique (R_{int}=0.0555), 2751 with I>2σ(I), R(F)[I>2σ(I)]=0.0464, wR(F^2)(I>4σ(I))=0.1253, R(F)[all data]=0.0468, wR(F^2)[all data]=0.1258, S=1.093, max/min Δρ in the final ΔF map: 1.18/-1.16 e·Å^{-3}.

Table S2. Crystallographic data and structure refinement details of complexes **1-25.**

1: $C_{25}H_{26}F_9LaN_{10}O_9S_3$, M_r=1016.65, orthorhombic, $Pca2_1$, a=10.9243(2)Å, b=17.2695(4)Å, c=19.9168(4)Å, V=3763.64(13)Å^3, Z=4, d_x=1.79 g·cm^{-3}, F(000)=2016, μ=11.31mm^{-1}, 10708 reflections collected, of which 6116 unique (R_{int}=0.029), 5432 with I>2σ(I), R(F)[I>2σ(I)]=0.046, wR(F^2)(I>4σ(I))=0.122, R(F)[all data]=0.052, wR(F^2)[all data]=0.128, S=1.05, max/min Δρ in the final ΔF map: 0.86/-0.46 e·Å^{-3}.

2: $C_{25}H_{26}F_9N_{10}O_9PrS_3$, M_r=1018.65, orthorhombic, $Pca2_1$, a=10.9258(3)Å, b=17.1974(4)Å, c=19.8714(6)Å, V=3733.74(18)Å^3, Z=4, d_x=1.81 g·cm^{-3}, F(000)=2024, μ=1.58mm^{-1}, 12868 reflections collected, of which 5629 unique (R_{int}=0.025), 4715 with I>2σ(I), R(F)[I>2σ(I)]=0.031, wR(F^2)(I>4σ(I))=0.077, R(F)[all data]=0.043, wR(F^2)[all data]=0.082, S=1.04, max/min Δρ in the final ΔF map: 0.56/-0.49 e·Å^{-3}. Flack parameter: 0.430(10).
2a: $C_{25}H_{26}F_9N_{10}O_9PrS_3$ C_2H_3N, M_r=1059.70, monoclinic, $P2_1$, a=8.9742(4)Å, b=14.0340(5)Å, c=15.8971(6)Å, β=92.838(4)°, V=1999.69(14)Å^3, Z=2, d_x=1.76g·cm^{-3}, F(000)=1056, μ=1.48mm^{-1}, 8138 reflections collected, of which 6021 unique (R_{int}=0.043), 5784 with I>2σ(I), R(F)[I>2σ(I)]=0.037, wR(F^2)(I>4σ(I))=0.087, R(F)[all data]=0.039, wR(F^2)[all data]=0.090, S=1.07, max/min Δρ in the final ΔF map: 2.42/-1.07e·Å^{-3}.
3: $C_{25}H_{26}F_9N_{10}NdO_9S_3$, M_r=1021.98, orthorhombic, $Pca2_1$, a=10.7762(2)Å, b=17.0625(2)Å, c=19.6569(3)Å, V=3614.29(10)Å^3, Z=4, d_x=1.88 g·cm^{-3}, F(000)=2028, μ=1.72mm^{-1}, 25948 reflections collected, of which 6680 unique (R_{int}=0.021), 6553 with I>2σ(I), R(F)[I>2σ(I)]=0.021, wR(F^2)(I>4σ(I))=0.052, R(F)[all data]=0.022, wR(F^2)[all data]=0.052, S=1.06, max/min Δρ in the final ΔF map: 0.75/-0.54 e·Å^{-3}. Flack parameter: 0.182(5).
4: $C_{25}H_{26}F_9N_{10}O_9S_3Sm$, M_r=1028.09, orthorhombic, $Pca2_1$, a=10.8093(5)Å, b=17.0375(5)Å, c=19.6847(5)Å, V=3625.2(2)Å^3, Z=4, d_x=1.88 g·cm^{-3}, F(000)=2036, μ=1.90mm^{-1}, 8618 reflections collected, of which 4954 unique (R_{int}=0.020), 4899 with I>2σ(I), R(F)[I>2σ(I)]=0.025, wR(F^2)(I>4σ(I))=0.066, R(F)[all data]=0.025, wR(F^2)[all data]=0.066, S=1.05, max/min Δρ in the final ΔF map: 1.02/-0.79 e·Å^{-3}. Flack parameter: 0.323(7).
5: $C_{25}H_{26}$ $EuF_9N_{10}O_9S_3$, M_r=1029.70, orthorhombic, $Pca2_1$, a=10.8953(2)Å, b=17.1060(3)Å, c=19.8121(5)Å, V=3692.24(13)Å^3, Z=4, d_x=1.85 g·cm^{-3}, F(000)=2040, μ=1.98mm^{-1}, 51185 reflections collected, of which 8358 unique (R_{int}=0.014), 7868 with I>2σ(I), R(F)[I>2σ(I)]=0.026, wR(F^2)(I>4σ(I))=0.066, R(F)[all data]=0.029, wR(F^2)[all data]=0.068, S=1.04, max/min Δρ in the final ΔF map: 1.04/-0.51 e·Å^{-3}. Flack parameter: 0.265(2).
6: $C_{25}H_{26}F_9GdN_{10}O_9S_3$, M_r=1034.99, orthorhombic, $Pca2_1$, a=10.9002(6)Å, b=17.0907(12)Å, c=19.8139(8)Å, V=3691.2(4)Å^3, Z=4, d_x=1.86 g·cm^{-3}, F(000)=2044, μ=2.08mm^{-1}, 9469 reflections collected, of which 5469 unique (R_{int}=0.041), 4714 with I>2σ(I), R(F)[I>2σ(I)]=0.055, wR(F^2)(I>4σ(I))=0.150, R(F)[all data]=0.065, wR(F^2)[all data]=0.157, S=1.07, max/min Δρ in the final ΔF map: 1.09/-0.80 e·Å^{-3}.
7: $C_{25}H_{34}F_3N_{10}O_5STb$ 2(CF_3O_3S), M_r=1100.74, monoclinic, $P2_1/n$, a=10.9638(4)Å, b=15.0249(7)Å, c=26.8438(15)Å, β=99.705(5)°, V=4358.7(4)Å^3, Z=4, d_x=1.68 g·cm^{-3}, F(000)=2192, μ=1.87mm^{-1}, 18343 reflections collected, of which 7646 unique (R_{int}=0.032), 6990 with I>2σ(I), R(F)[I>2σ(I)]=0.096, wR(F^2)(I>4σ(I))=0.206, R(F)[all data]=0.103, wR(F^2)[all data]=0.209, S=1.13, max/min Δρ in the final ΔF map: 9.53/-3.60 e·Å^{-3}.
7a: $C_{26}H_{26}F_6N_{11}O_6S_2Tb$ CF_3O_3S, M_r=1074.69, monoclinic, $P2_1/c$, a=19.0497(5)Å, b=10.3198(2)Å, c=21.3425(5)Å, β=102.668(2)°, V=4093.57(17)Å^3, Z=4, d_x=1.74 g·cm^{-3}, F(000)=2124, μ=10.86mm^{-1}, 16653 reflections collected, of which 7381 unique (R_{int}=0.023), 6405 with I>2σ(I), R(F)[I>2σ(I)]=0.069, wR(F^2)(I>4σ(I))=0.206, R(F)[all data]=0.076, wR(F^2)[all data]=0.211, S=1.45, max/min Δρ in the final ΔF map: 1.71/-1.26 e·Å^{-3}.
8: $C_{25}H_{34}DyF_3N_{10}O_5S$ 2(CF_3O_3S), M_r=1104.32, monoclinic, $P2_1/n$, a=10.9170(3)Å, b=14.9827(3)Å, c=26.8953(10)Å, β=100.184(3)°, V=4329.9(2)Å^3, Z=4, d_x=1.69 g·cm^{-3}, F(000)=2196, μ=1.97mm^{-1}, 38766 reflections collected, of which 7596 unique (R_{int}=0.081), 5550 with I>2σ(I), R(F)[I>2σ(I)]=0.087, wR(F^2)(I>4σ(I))=0.176, R(F)[all data]=0.118, wR(F^2)[all data]=0.183, S=1.71, max/min Δρ in the final ΔF map: 5.13/-2.64 e·Å^{-3}.
9: $C_{26}H_{26}F_6HoN_{11}O_6S_2$ CF_3O_3S, M_r=1083.72, monoclinic, $P2_1/c$, a=18.7750(7)Å, b=10.2574(2)Å, c=21.0038(6)Å, β=101.760(3)°, V=3960.1(2)Å^3, Z=4, d_x=1.82 g·cm^{-3}, F(000)=2144, μ=2.26mm^{-1}, 14768 reflections collected, of which 6967 unique (R_{int}=0.017), 6291 with I>2σ(I), R(F)[I>2σ(I)]=0.053, wR(F^2)(I>4σ(I))=0.139, R(F)[all data]=0.059, wR(F^2)[all data]=0.141, S=1.97, max/min Δρ in the final ΔF map: 2.87/-2.26 e·Å^{-3}.
10: $C_{25}H_{34}ErF_3N_{10}O_5S$ 2(CF_3O_3S), M_r=1109.08 , monoclinic, $P2_1/n$, a=10.9049(4)Å, b=15.0238(4)Å, c=27.3563(9)Å, β=100.350(4)°, V=4408.9(3)Å^3, Z=4, d_x=1.67 g·cm^{-3}, F(000)=2204, μ=2.15mm^{-1}, 18023 reflections collected, of which 9184 unique (R_{int}=0.046), 8398 with I>2σ(I), R(F)[I>2σ(I)]=0.070, wR(F^2)(I>4σ(I))=0.170, R(F)[all data]=0.075, wR(F^2)[all data]=0.173, S=1.12, max/min Δρ in the final ΔF map: 5.67/-3.19e·Å^{-3}.
11: $C_{24}H_{26}F_6N_{10}O_6S_2Yb$ CF_3O_3S, M_r=1050.78, triclinic, $P\bar{1}$, a=11.3018(5)Å, b=13.3845(6)Å, c=14.5613(4)Å, α=96.292(3)°, β=99.214(3)°, γ=107.796(4)°, V=2040.55(15)Å^3, Z=2, d_x=1.71g·cm^{-3}, F(000)=1034, μ=2.54mm^{-1}, 21875 reflections collected, of which 7183 unique (R_{int}=0.039), 6382 with I>2σ(I), R(F)[I>2σ(I)]=0.056, wR(F^2)(I>4σ(I))=0.159, R(F)[all data]=0.062, wR(F^2)[all data]=0.163, S=1.31, max/min Δρ in the final ΔF map: 3.23/-1.11e·Å^{-3}.
13: $C_{12}H_{17}LaN_8O_{10}$ C_2H_3N, M_r=613.30, triclinic, $P\bar{1}$, a=8.2733(4)Å, b=11.4426(7)Å, c=13.5163(7)Å, α=109.919(6)°, β=106.972(4)°, γ=93.483(4)°, V=1132.21(12)Å^3, Z=2, d_x=1.80g·cm^{-3}, F(000)=608, μ=1.96mm^{-1}, 5084 reflections collected, of which 3393 unique (R_{int}=0.019), 3317 with I>2σ(I), R(F)[I>2σ(I)]=0.022,

$wR(F^2)(I>4\sigma(I))=0.068$, R(F)[all data]=0.023, $wR(F^2)$[all data]=0.069, S=1.12, max/min Δρ in the final ΔF map: 0.66/-1.02e·Å^{-3}.
14: $C_{12}H_{17}N_8O_{10}Pr\cdot\frac{1}{2}(CH_4O)$, M_r=590.27, triclinic, $P\bar{1}$, a=8.1238(3)Å, b=10.5711(7)Å, c=12.6360(5)Å, α=99.359(4)°, β=97.224(4)°, γ=100.751(4)°, V=1038.18(9)Å^3, Z=2, d_x=1.89g·cm^{-3}, F(000)=586, μ=2.42mm^{-1}, 6734 reflections collected, of which 4006 unique (R_{int}=0.019), 3893 with I>2σ(I), R(F)[I>2σ(I)]=0.023, $wR(F^2)(I>4\sigma(I))=0.062$, R(F)[all data]=0.024, $wR(F^2)$[all data]=0.063, S=1.08, max/min Δρ in the final ΔF map: 1.07/-0.63e·Å^{-3}.
15: $C_{12}H_{17}N_8NdO_{10}$ C_2H_3N, M_r=618.63, triclinic, $P\bar{1}$, a=8.3168(5)Å, b=11.3880(6)Å, c=13.4939(8)Å, α=110.119(5)°, β=107.600(5)°, γ=92.758(5)°, V=1127.23(12)Å^3, Z=2, d_x=1.82g·cm^{-3}, F(000)=614, μ=2.37mm^{-1}, 7629 reflections collected, of which 4261 unique (R_{int}=0.012), 4103 with I>2σ(I), R(F)[I>2σ(I)]=0.016, $wR(F^2)(I>4\sigma(I))=0.038$, R(F)[all data]=0.017, $wR(F^2)$[all data]=0.038, S=1.08, max/min Δρ in the final ΔF map: 0.47/-0.45e·Å^{-3}.
16: $C_{11}H_{15}N_8O_{10}Sm\cdot CH_4O$, M_r=601.70, triclinic, $P\bar{1}$, a=8.1537(3)Å, b=10.4239(4)Å, c=12.3673(3)Å, α=96.710(3)°, β=98.034(3)°, γ=100.381(4)°, V=1012.84(6)Å^3, Z=2, d_x=1.97g·cm^{-3}, F(000)=594, μ=2.98mm^{-1}, 7077 reflections collected, of which 4169 unique (R_{int}=0.020), 3879 with I>2σ(I), R(F)[I>2σ(I)]=0.021, $wR(F^2)(I>4\sigma(I))=0.045$, R(F)[all data]=0.024, $wR(F^2)$[all data]=0.046, S=1.04, max/min Δρ in the final ΔF map: 0.62/-0.50e·Å^{-3}.
17: $C_{11}H_{15}EuN_8O_{10}\cdot CH_4O$, M_r=603.31, triclinic, $P\bar{1}$, a=8.1426(4) Å, b=10.4679(8) Å, c=12.4743(7) Å, α=98.188(6) °, β=97.531(4)°, γ=100.576(5)°, V=1020.95(11) Å^3, Z=2, d_x=1.96g·cm^{-3}, F(000)=596, μ=3.14mm^{-1}, 7292 reflections collected, of which 4237 unique (R_{int}=0.023), 3940 with I>2σ(I), R(F)[I>2σ(I)]=0.035, $wR(F^2)(I>4\sigma(I))=0.081$, R(F)[all data]=0.039, $wR(F^2)$[all data]=0.083, S=1.07, max/min Δρ in the final ΔF map: 2.47/-1.89e·Å^{-3}.
18: $C_{12}H_{17}GdN_8O_{10}$ C_2H_3N, M_r=631.64, triclinic, $P\bar{1}$, a=8.2937(17)Å, b=11.3355(15)Å, c=13.441(3)Å, α=110.013(16)°, β=107.641(18)°, γ=92.604(14)°, V=1115.7(4)Å^3, Z=2, d_x=1.88g·cm^{-3}, F(000)=622, μ=3.04mm^{-1}, 7965 reflections collected, of which 4601 unique (R_{int}=0.024), 4217 with I>2σ(I), R(F)[I>2σ(I)]=0.024, $wR(F^2)(I>4\sigma(I))=0.055$, R(F)[all data]=0.028, $wR(F^2)$[all data]=0.056, S=1.05, max/min Δρ in the final ΔF map: 1.19/-0.77e·Å^{-3}.
19: $C_{11}H_{15}N_8O_{10}TbCH_4O$, M_r=610.27, triclinic, $P\bar{1}$, a=8.2400(4)Å, b=10.5276(6)Å, c=12.3755(6)Å, α=98.043(4)°, β=96.749(4)°, γ=100.129(5)°, V=1035.23(9)Å^3, Z=2, d_x=1.96g·cm^{-3}, F(000)=600, μ=17.49mm^{-1}, 7534 reflections collected, of which 4161 unique (R_{int}=0.047), 4034 with I>2σ(I), R(F)[I>2σ(I)]=0.045, $wR(F^2)(I>4\sigma(I))=0.130$, R(F)[all data]=0.045, $wR(F^2)$[all data]=0.131, S=1.09, max/min Δρ in the final ΔF map: 1.87/-2.25e·Å^{-3}.
20: $C_{11}H_{15}DyN_8O_{10}$ CH_4O, M_r=613.85, triclinic, $P\bar{1}$, a=8.2029(7)Å, b=10.4813(9)Å, c=12.4024(7)Å, α=97.826(6)°, β=96.891(6)°, γ=100.152(7)°, V=1028.45(14)Å^3, Z=2, d_x=1.98g·cm^{-3}, F(000)=602, μ=3.71mm^{-1}, 7224 reflections collected, of which 4207 unique (R_{int}=0.017), 3955 with I>2σ(I), R(F)[I>2σ(I)]=0.021, $wR(F^2)(I>4\sigma(I))=0.048$, R(F)[all data]=0.024, $wR(F^2)$[all data]=0.049, S=1.06, max/min Δρ in the final ΔF map: 0.60/-0.47e·Å^{-3}.
21: $C_{12}H_{17}HoN_8O_{10}$ C_2H_3N, M_r=639.32, triclinic, $P\bar{1}$, a=8.2808(4)Å, b=11.2432(6)Å, c=13.2986(9)Å, α=68.357(6)°, β=72.061(5)°, γ=87.716(4)°, V=1091.08(12)Å^3, Z=2, d_x=1.95g·cm^{-3}, F(000)=628, μ=3.70mm^{-1}, 8017 reflections collected, of which 4528 unique (R_{int}=0.026), 4302 with I>2σ(I), R(F)[I>2σ(I)]=0.026, $wR(F^2)(I>4\sigma(I))=0.064$, R(F)[all data]=0.028, $wR(F^2)$[all data]=0.066, S=1.09, max/min Δρ in the final ΔF map: 1.47/-1.50e·Å^{-3}.
22: $C_{11}H_{15}ErN_8O_{10}$, M_r=586.57, triclinic, $P\bar{1}$, a=8.3705(7)Å, b=9.3039(7)Å, c=12.7182(9)Å, α=102.222(6)°, β=103.692(7)°, γ=102.763(6)°, V=901.39(13)Å^3, Z=2, d_x=2.16g·cm^{-3}, F(000)=570, μ=4.73mm^{-1}, 5555 reflections collected, of which 3145 unique (R_{int}=0.068), 2826 with I>2σ(I), R(F)[I>2σ(I)]=0.057, $wR(F^2)(I>4\sigma(I))=0.149$, R(F)[all data]=0.065, $wR(F^2)$[all data]=0.154, S=1.23, max/min Δρ in the final ΔF map: 4.16/-2.24e·Å^{-3}.
23: $C_{12}H_{17}N_8O_{10}TmC_{11}H_{14}N_5\cdot NO_3$, M_r=880.55, triclinic, $P\bar{1}$, a=8.3950(4)Å, b=12.7332(6)Å, c=16.9061(9)Å, α=71.362(5)°, β=80.611(4)°, γ=76.595(4)° V=1657.96(15)Å^3, Z=2, d_x=1.76g·cm^{-3}, F(000)=880, μ=5.76mm^{-1}, 11642 reflections collected, of which 6651 unique (R_{int}=0.043), 6370 with I>2σ(I), R(F)[I>2σ(I)]=0.059, $wR(F^2)(I>4\sigma(I))=0.163$, R(F)[all data]=0.061, $wR(F^2)$[all data]=0.164, S=1.10, max/min Δρ in the final ΔF map: 1.72/-3.09e·Å^{-3}.
24: $C_{12}H_{17}N_8O_{10}Yb$ C_2H_3N, M_r=647.43, triclinic, $P\bar{1}$, a=8.1752(5)Å, b=11.5352(9)Å, c=13.1045(10)Å, α=66.989(7)°, β=72.978(6)°, γ=85.535(5)°, V=1086.69(15)Å^3, Z=2, d_x=1.98g·cm^{-3}, F(000)=634, μ=4.38mm^{-1}, 4347 reflections collected, 3960 with I>2σ(I), R(F)[I>2σ(I)]=0.049, $wR(F^2)(I>4\sigma(I))=0.159$, R(F)[all data]=0.058,

$wR(F^2)$[all data]=0.162, S=1.39, max/min Δρ in the final ΔF map: 3.27/-5.07e·Å^{-3}.
25: $C_{13}H_{19}LuN_8O_{10}S·CH_3CN$, M_r=695.44, orthorhombic, Pna2, a=23.9529(11)Å, b=11.3128(4)Å, c=9.2768(4)Å, α=90°, β=90°, γ=90°, V=2513.77(18)Å^3, Z=4, d_x=1.838g·cm^{-3}, F(000)=1368, μ=8.900mm^{-1}, 9005 reflections collected, of which 4510 unique (R_{int}=0.0523), 4342 with I>2σ(I), R(F)[I>2σ(I)]=0.0531, $wR(F^2)$(I>4σ(I))=0.1517, R(F)[all data]=0.0547, $wR(F^2)$[all data]=0.1540, S=1.084, max/min Δρ in the final ΔF map: 2.22/-1.80e·Å^{-3}.

Table S3. Crystallographic data and structure refinement details of complexes **Tb-perchlorate** and **Eu-hydrogen.**

Tb-perchlorate: $C_{24}H_{31}ClN_{11}O_5Tb^{2+}$ ·2(ClO_4^-), M_r=946.87, triclinic, $P\bar{1}$, a=9.0968(9)Å, b=11.9590(8)Å, c=17.1192(12)Å, α=86.084(6)°, β=75.282(7)°, γ=83.710(7)° V=1788.8(3)Å^3, Z=2, d_x=1.758g·cm^{-3}, F(000)=944, μ=2.277mm^{-1}, 11546 reflections collected, of which 6235 unique (R_{int}=0.1416), 2982 with I>2σ(I), R(F)[I>2σ(I)]=0.0745, $wR(F^2)$(I>4σ(I))=0.1365, R(F)[all data]=0.1362, $wR(F^2)$[all data]=0.1654, S=0.905, max/min Δρ in the final ΔF map: 1.47/-1.21e·Å^{-3}.
Eu-hydrogen: $C_{25}H_{30}EuF_9N_{10}O_{11}^+·CF_3SO_3^-·CH_3OH$, M_r=1065.73, monoclinic, $P2_1/c$, a=13.59487(17)Å, b=15.49254(18)Å, c=17.9886(3)Å, α=90°, β=92.7582(12)°, γ=90° V=3784.35(9)Å^3, Z=4, d_x=1.871g·cm^{-3}, F(000)=2120, μ=1.936mm^{-1}, 38298 reflections collected, of which 8448 unique (R_{int}=0.0369), 7065 with I>2σ(I), R(F)[I>2σ(I)]=0.0269, $wR(F^2)$(I>4σ(I))=0.0517, R(F)[all data]=0.0393, $wR(F^2)$[all data]=0.0553, S=1.044, max/min Δρ in the final ΔF map: 0.66/-0.57e·Å^{-3}.

Table S4. Selected Bond Distances (Å) for complexes **1-6**.

Bond	1	2	3	4	5	6
Ln-N14A	2.64(1)	2.575(8)	2.537(4)	2.522(6)	2.508(6)	2.50(2)
Ln-N14B	2.56(1)	2.551(9)	2.551(4)	2.515(6)	2.518(7)	2.51(2)
Ln-N1A	2.640(8)	2.589(5)	2.573(3)	2.542(4)	2.549(4)	2.54(1)
Ln-N1B	2.65(1)	2.594(6)	2.564(4)	2.553(5)	2.532(5)	2.53(1)
Ln-N8A	2.727(7)	2.676(5)	2.650(3)	2.637(4)	2.621(4)	2.61(1)
Ln-N8B	2.735(8)	2.691(5)	2.652(3)	2.628(3)	2.625(4)	2.61(1)
Ln-O13C	2.561(7)	2.528(4)	2.504(2)	2.502(3)	2.504(3)	2.507(9)
Ln-O13D	2.53(1)	2.505(6)	2.471(3)	2.457(4)	2.441(4)	2.43(1)
Ln-O13E	2.53(1)	2.485(6)	2.483(3)	2.447(4)	2.446(4)	2.44(1)

Table S5. Selected Bond Distances (Å) for complexes **7-11**.

Bond	7	8	10	Bond	9	11
Ln-N14A	2.49(1)	2.478(8)	2.465(6)	**Ln-N14A**	2.454(5)	2.390(9)
Ln-N14B	2.484(9)	2.468(9)	2.445(6)	**Ln-N14B**	2.447(5)	2.402(6)
Ln-N1A	2.559(8)	2.539(7)	2.520(7)	**Ln-N1A**	2.545(5)	2.475(8)
Ln-N1B	2.563(9)	2.534(8)	2.515(6)	**Ln-N1B**	2.522(5)	2.470(7)
Ln-N8A	2.607(9)	2.592(8)	2.572(6)	**Ln-N1E**	2.543(6)	-
Ln-N8B	2.576(9)	2.570(8)	2.557(5)	**Ln-N8A**	2.552(4)	2.480(7)
Ln-O13C	2.355(9)	2.361(8)	2.331(6)	**Ln-N8B**	2.555(7)	2.511(7)
Ln-O1D	2.432(8)	2.441(8)	2.390(5)	**Ln-O11C**	2.344(4)	2.255(6)
Ln-O1E	2.461(9)	2.411(7)	2.434(6)	**Ln-O11D**	2.328(5)	2.235(5)

Table S6. Selected Bond Distances (Å) for complexes **2a** and **7a**.

Bond	2a	Bond	7a
Ln-N14A	2.605(7)	**Ln-N14A**	2.480(5)
Ln-N14B	2.523(5)	**Ln-N14B**	2.468(6)
Ln-N1A	2.572(7)	**Ln-N1A**	2.577(6)
Ln-N1B	2.580(7)	**Ln-N1B**	2.544(6)
Ln-N8A	2.667(6)	**Ln-N1D**	2.572(8)
Ln-N8B	2.675(6)	**Ln-N8A**	2.577(6)
Ln-O13C	2.484(5)	**Ln-N8B**	2.579(8)
Ln-O13D	2.524(3)	**Ln-O11E**	2.368(5)
Ln-O13E	2.486(5)	**Ln-O13C**	2.366(5)

Table S7. Selected Bond Distances (Å) for complexes **13**, **15-18**, **22** and **24**.

Bond	13	15	16	17	18	22	24
Ln-N14A	2.613(3)	2.558(2)	2.515(2)	2.511(4)	2.510(3)	2.41(1)	2.418(5)
Ln-N1A	2.661(2)	2.608(2)	2.556(2)	2.548(4)	2.565(2)	2.45(1)	2.460(8)
Ln-N8A	2.688(2)	2.617(2)	2.572(2)	2.555(4)	2.570(3)	2.506(8)	2.486(8)
Ln-O11B	2.617(2)	2.613(2)	2.502(2)	2.476(4)	2.539(2)	2.460(8)	2.440(5)
Ln-O11C	2.596(3)	2.531(2)	2.507(2)	2.494(3)	2.474(3)	2.426(9)	2.451(7)
Ln-O11D	2.669(2)	2.565(1)	2.578(2)	2.572(3)	2.580(3)	2.302(9)	-
Ln-O12B	2.592(2)	2.553(1)	2.578(2)	2.567(4)	2.501(2)	2.382(7)	2.402(6)
Ln-O12C	2.656(2)	2.603(1)	2.576(2)	2.549(4)	2.574(2)	2.436(8)	2.382(7)
Ln-O12D	2.606(2)	2.544(1)	2.526(2)	2.519(4)	2.510(2)	-	2.251(5)
Ln-O1E	2.504(3)	2.449(2)	2.418(2)	2.426(3)	2.400(3)	2.357(6)	2.331(5)

Table S8. Selected Bond Distances (Å) for complexes **14** and **19-21**.

Bond	14	19	20	21
Ln-N14A	2.567(3)	2.490(5)	2.469(3)	2.468(2)
Ln-N1A	2.595(2)	2.538(5)	2.508(3)	2.523(3)
Ln-N8A	2.615(2)	2.535(4)	2.524(2)	2.500(3)
Ln-O12B	2.600(2)	2.562(5)	2.563(2)	2.540(4)
Ln-O12C	2.593(2)	2.573(5)	2.567(3)	2.447(2)
Ln-O12D	2.540(2)	2.490(4)	2.466(2)	2.422(2)
Ln-O13B	2.583(2)	2.485(5)	2.474(2)	2.453(3)
Ln-O13C	2.532(2)	2.440(5)	2.442(3)	2.503(3)
Ln-O13D	2.576(2)	2.550(5)	2.559(2)	2.530(2)
Ln-O1E	2.492(2)	2.398(4)	2.377(2)	2.358(2)

Table S9. Selected Bond Distances (Å) for complexes **23** and **25**.

Bond	23	Bond	25
Ln-N14A	2.486(6)	**Ln**-N1A	2.40(1)
Ln-N1A	2.389(5)	**Ln**-N10A	2.43(1)
Ln-N8A	2.545(5)	**Ln**-N7A	2.53(1)
Ln-O12B	2.413(5)	**Ln**-O1C	2.563(9)
Ln-O12C	2.345(4)	**Ln**-O2C	2.371(9)
Ln-O13B	2.462(5)	**Ln**-O2B	2.38(1)
Ln-O13C	2.465(6)	**Ln**-O1B	2.46(1)
Ln-O11C	2.279(9)	**Ln**-O1D	2.28(1)
Ln-O1D	2.345(5)	**Ln**-O1E	2.240(8)

Supporting Figures

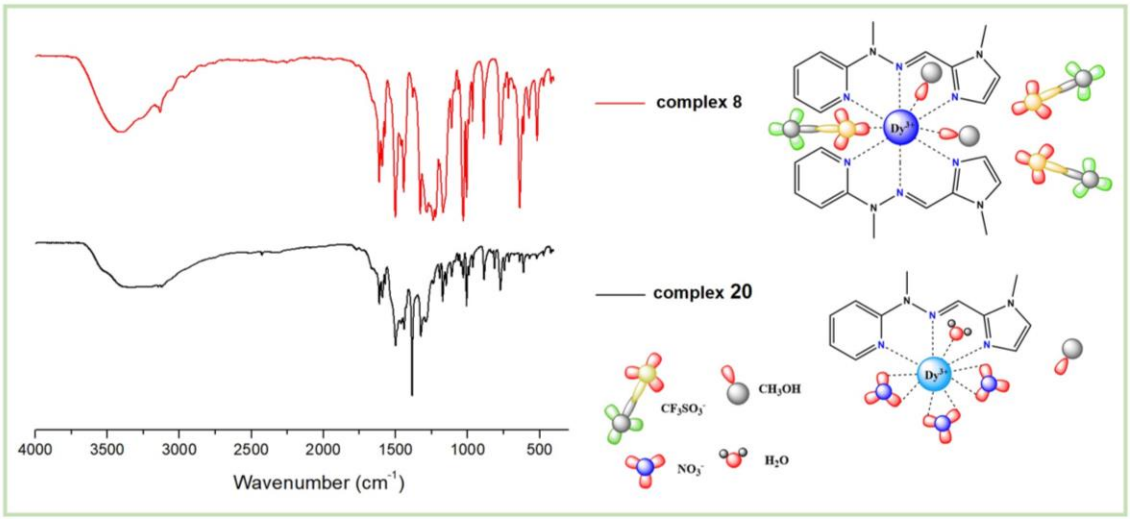

Figure S1. Representative FT-IR spectra of complexes from the triflate and nitrate series along their schematic coordination modes.

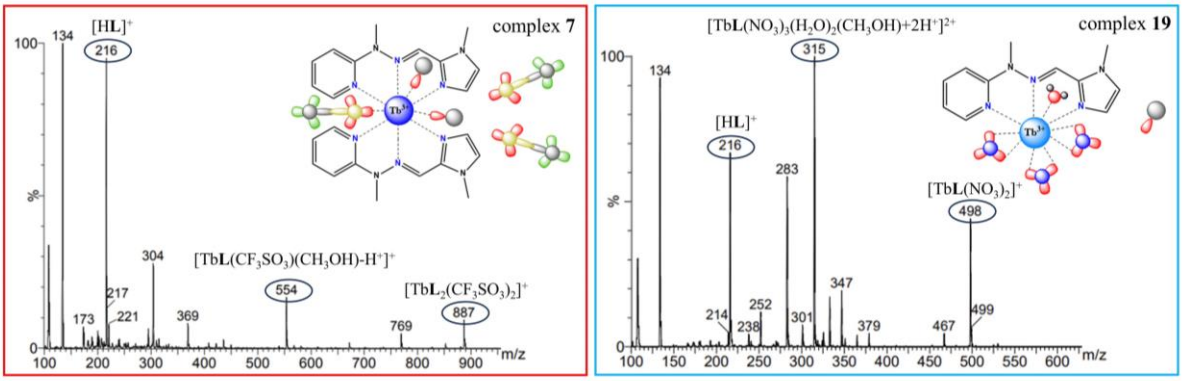

Figure S2. Representative mass spectra of complexes from the triflate and nitrate series along their schematic coordination modes.

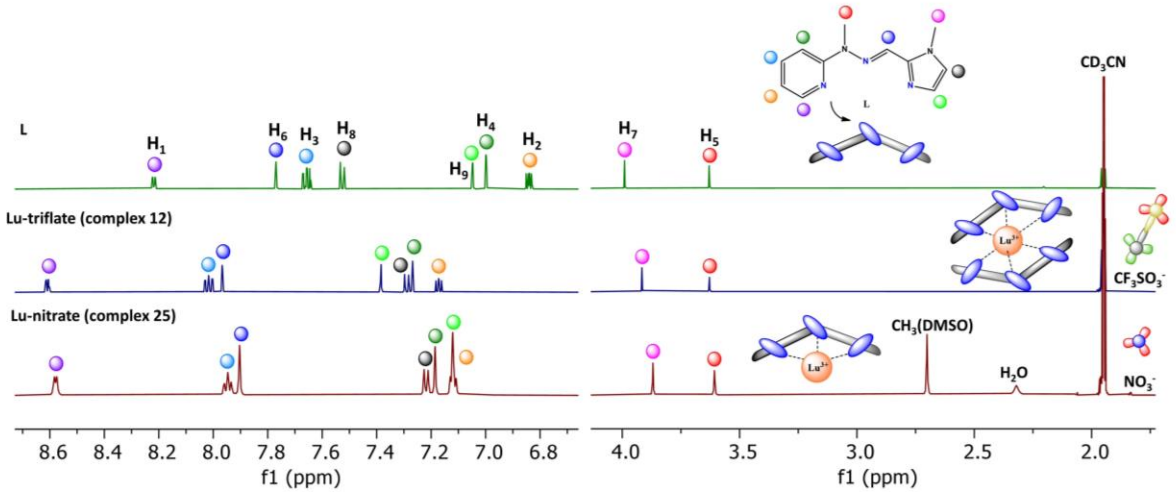

Figure S3. The comparison of ^{1}H NMR spectra of ligand **L** and the diamagnetic Lu(III) triflate (**12**) and Lu(III) nitrate (**25**) complexes.

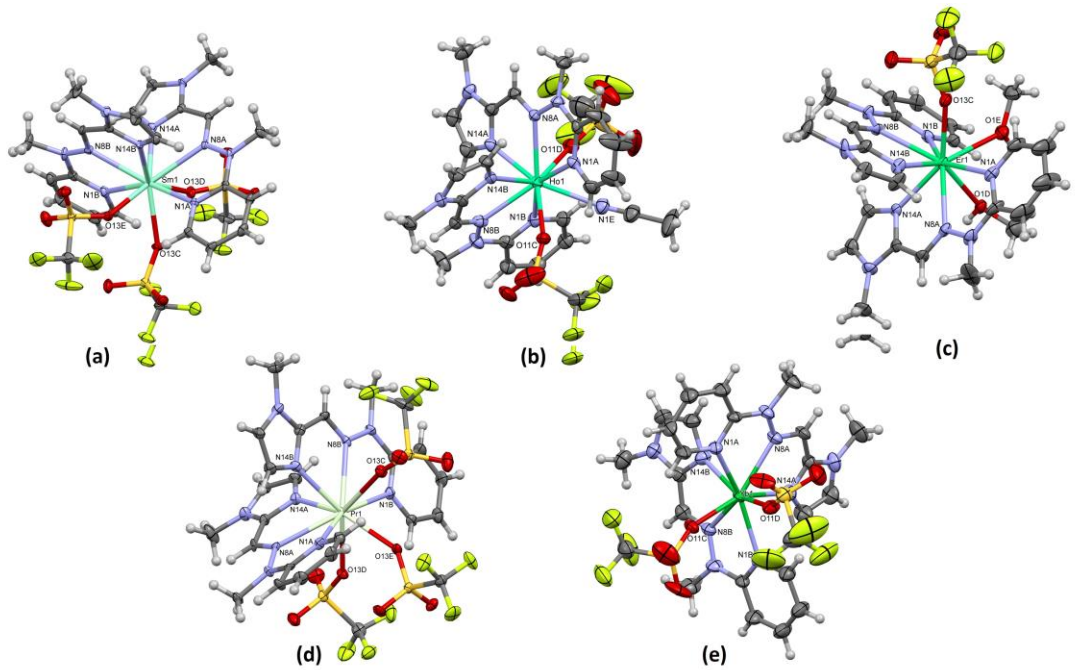

Figure S4. Perspective view one of the isostructural: (a) Pca2$_1$ complexes (**4**), (b) P2$_1$/c complexes (**9**), (c) P2$_1$/n (**10**) complexes and of the single complexes (d) P2$_1$ (**2a**), (e) P$\bar{1}$ (**11**); ellipsoids are drawn at the 50% probability level, hydrogen atoms are depicted as spheres of arbitrary radii.

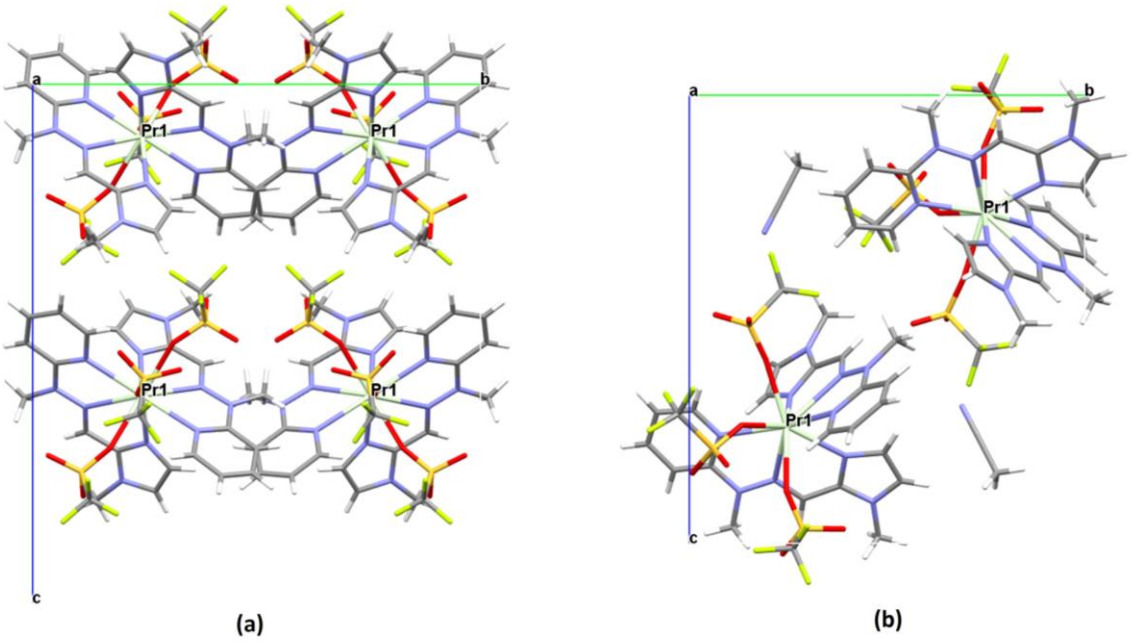

Figure S5. Crystal packing of complexes **2** (left) and **2a** (right).

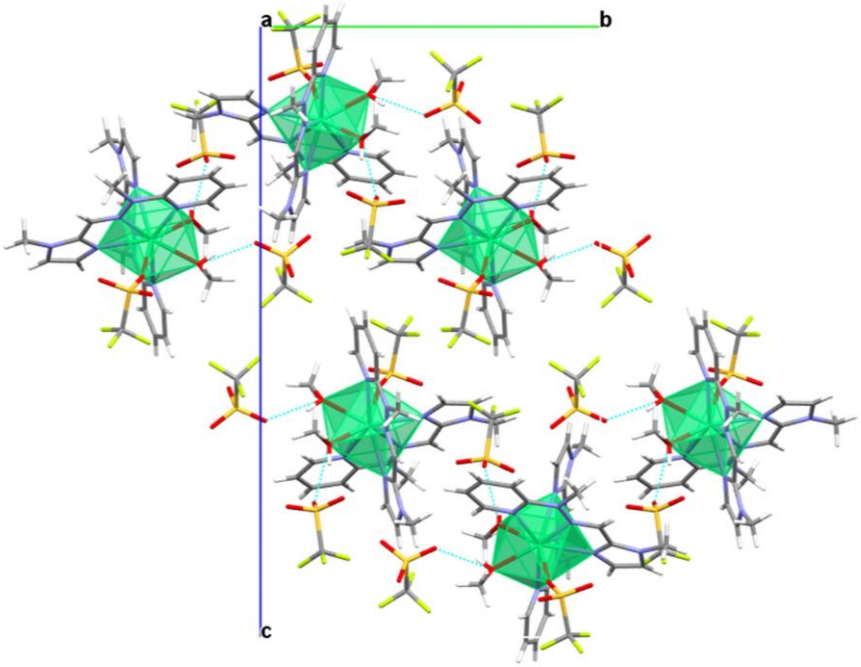

Figure S6. Supramolecular structure created by molecule **10** as an example of motifs present in dicationic complexes from triflate series as seen along a axis. Thin blue lines show hydrogen bonds.

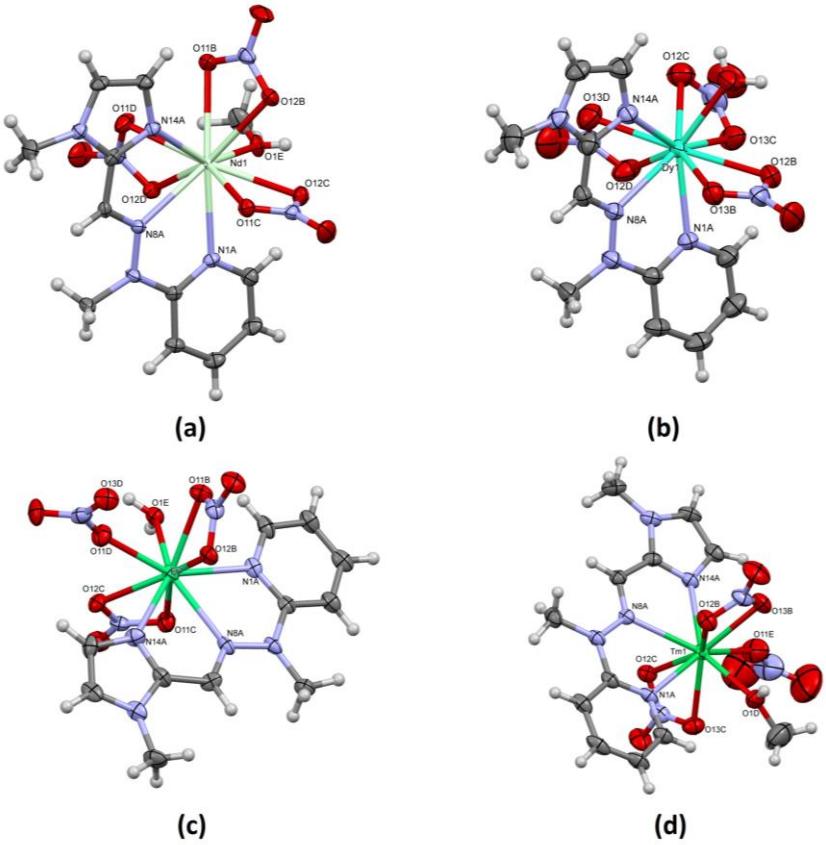

Figure S7. Perspective view of the representative examples from the nitrate series of (a) Nd(III) complex (**15**), (b) Dy(III) complex (**20**), (c) Er(III) complex (**22**) and (d) Tm(III) complex (**23**); ellipsoids are drawn at the 50% probability level, hydrogen atoms are depicted as spheres of arbitrary radii.

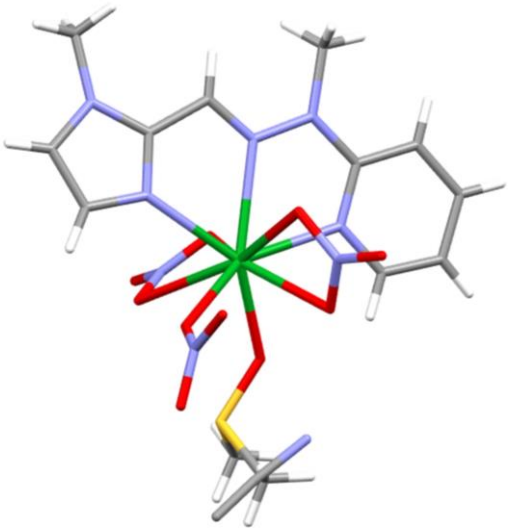

Figure S8. Crystal structure of complex **25** with lutetium(III) metal ion in the nitrate series.

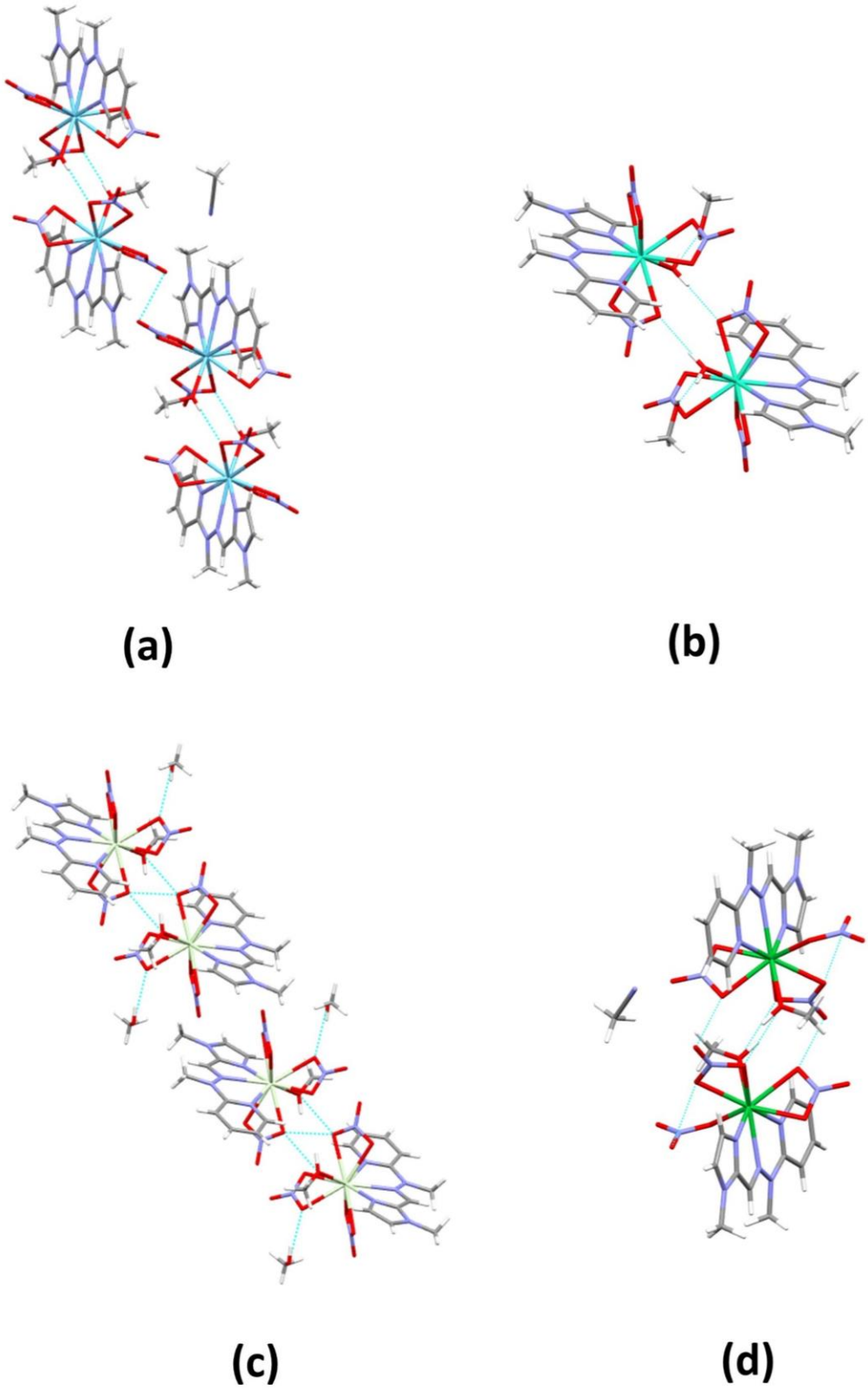

Figure S9. A comparison of the supramolecular structures created by molecules of **13** (a), **20** (b), **14** (c) and **24** (d) as seen along a axis. Thin blue lines show hydrogen bonds.

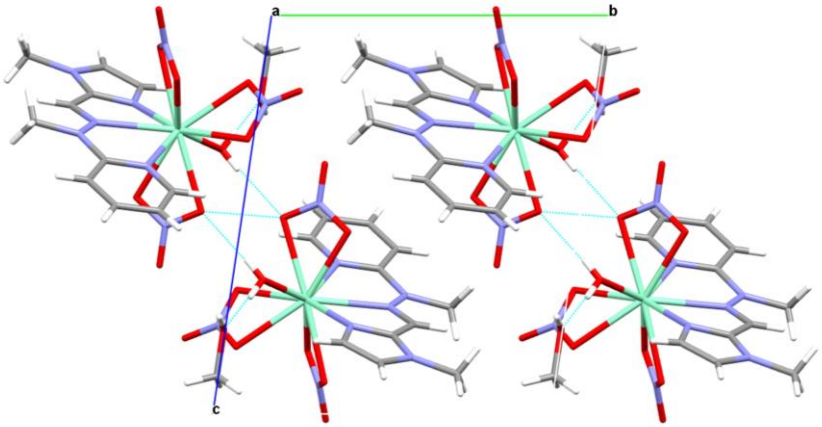

Figure S10. Representative example of the supramolecular structure created by complex **16**.

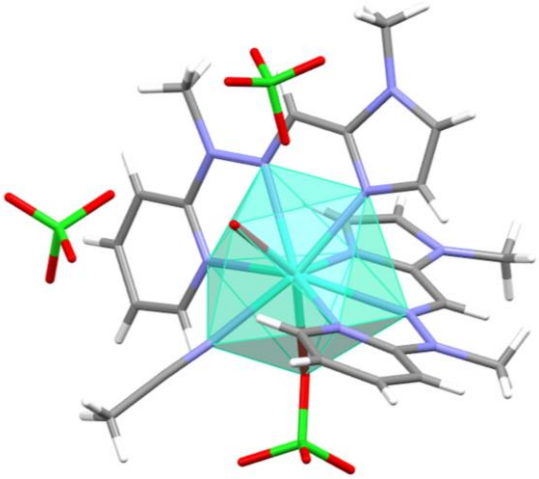

Figure S11. Crystal structure of complex **Tb-perchlorate** with terbium(III) metal ion and perchlorate counterions.